2008 IEEE International Conference on
Robotics and Automation
Pasadena, CA, USA, May 19-23, 2008

ROCR: Dynamic Vertical Wall Climbing with a Pendular Two-Link Mass-Shifting Robot

Samuel Jensen-Segal, Steven Virost and William R. Provancher

Abstract— **We present a novel bio-inspired dynamic climbing robot, with a recursive name: ROCR is an Oscillating Climbing Robot. ROCR is a pendular two-link, serial chain robot that utilizes alternating hand-holds and an actuated tail to propel itself upward in a climbing style based on observation of human climbers and brachiating gibbons. ROCR's bio-inspired oscillating climbing strategy is simple and efficient. This robot is intended for autonomous surveillance and inspection on sheer vertical surfaces. Potential locomotion gait strategies were investigated in simulation using Working Model 2D. Strategy comparisons were drawn on a basis of climbing rate and energy efficiency. Simulation results show the feasibility and relative merits of these climbing gait strategies and compare them to the potential energy gained while climbing. A first generation ROCR design, having physical parameters based on simulation analysis, that utilizes actuated permanent magnet grippers and a geared-motor actuated tail was fabricated. Magnetic grippers are used for this initial prototype to facilitate investigating the robots climbing efficiency. Several climbing gaits which showed promise in simulation were implemented in the prototype. ROCR is a lightweight, flexible, self-contained robot with on-board microcontroller, tilt and acceleration sensing, power supply and wireless communication. We conclude with plans to evolve the simulation and design of the robot and plans for testing the prototype.**

I. INTRODUCTION

Robots can be designed to work in hostile [1], dangerous [2] or challenging environments [3]. Much progress has been made by small ground traversing robots in traveling over rough terrain. Climbing robots can be used to perform inspection [4], [5], [6], [7], service [8], and surveillance [9], [10] on shear vertical or near-vertical surfaces. Climbing robots face a variety of challenges distinct from those faced by ground traversing robots. Such challenges include needing to fully lift their entire mass in order to make vertical progress as in the case of 'pull-up' style climbers, physically holding onto a vertical surface, maneuvering laterally or over surface features, and self-orienting in the vertical plane. In recent years, climbing robots have become lighter, more adaptable to a wide variety of surfaces, and much more sophisticated in their functional capabilities. These advances have been driven by improved manufacturing techniques, increased microcontroller computational power, and novel strategies for climbing. Climbing robots make use of many gripping tools including suction systems [11], [12], directional adhesives [9], [13], [14], magnets [15], [16], [17], and gripping spines [18], [19] to hold or grip vertical surfaces. These robots employ many types of mechanical actuation devices to facilitate their climbing strategies, including wheels [10], tracks [6], actuated arms [4], [20], vacuum adhesion systems [21], [22], pneumatically actuated systems [2], and cables [23]. Many of these climbing strategies have been inspired by observation of the natural world. The core innovations of ROCR, its energy-efficient climbing strategy and simple mechanical design, arise from observing mass shifting in human climbers and brachiative motion in animals. The resultant, body-oscillating, mass-shifting climbing strategy is very energy efficient and enables a wide range of climbing gaits to suit different surfaces, tasks, and power or weight requirements. While pendular mass shifting has been explored as a means of dynamic wall climbing [19], ROCR focuses on the benefits this climbing strategy offers in terms of energy efficiency and mechanical simplicity.

Proficient human climbers take advantage of both subtle and dramatic mass shifting to gain elevation with minimal physical effort. A simple lateral body movement prior to changing handholds often enables a human climber to reach higher with less pull-up effort. Human climbers often engage in dramatic mass shifting in preparation for highly dynamic climbing motions, essentially winding-up and then releasing their potential energy (PE) into a large vertical gain.

Brachiation is most notably employed by gibbons when they swing from one handhold to the next in a very dynamic pattern of gripping and swinging [24]. Brachiative motion strings together a sequence of pendular paths with coordinated grip changes to achieve lateral motion. In this method of lateral swinging motion, very little input energy is required to maintain physical progress [25], [26]. ROCR turns standard gibbon brachiation vertical, combining it with human style mass shifting into a tail-swinging body-oscillating scansorial climbing strategy. As expected with a pendular system, maximum efficiency can be achieved by targeting the natural frequency of the system, as has been previously done with ground traversing robots [28].

By mimicking climbing strategies employed by human climbers and animals, a simple, energy efficient climbing strategy has been developed. ROCR uses precise mass shifts, affected by a carefully controlled tail motions, developed from optimized simulations, to raise one hand at a time. Combining and integrating these behaviors enables ROCR to climb efficiently with a minimum of moving parts.

In order to demonstrate the significance of this new climbing strategy, an overview of the physical design of the robot

W. R. Provancher is with Faculty of Mechanical Engineering, University of Utah, Salt Lake City, UT 84112 wil@mech.utah.edu

S. Jensen-Segal and S. Virost are with the Department of Mechanical Engineering, University of Utah, Salt Lake City, UT 84112, sam.segal@mech.utah.edu, virost@mech.utah.edu

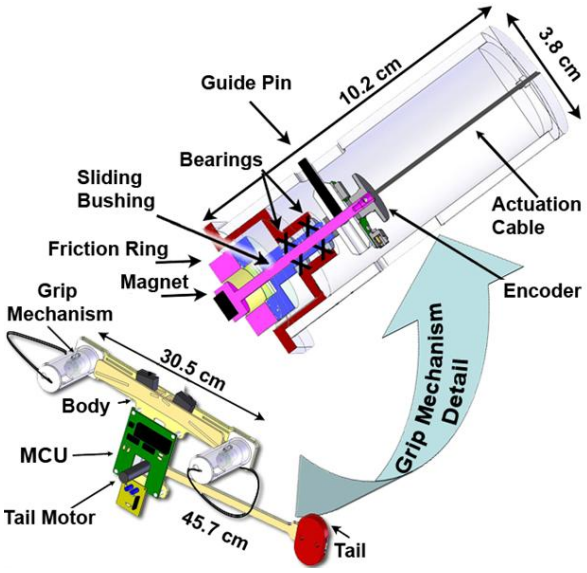

Fig. 1. Front view of ROCR shown small with detail view of gripping mechanism. Body (30.5 cm X 20.3 cm), tail (45.7 cm long) with tail mass. Gripping mechanisms shown at ends of T-shaped body. Total robot mass is approximately 0.6 kg with a total body length of 57 cm. In the detailed section view of magnetic grip assembly, note magnetic piston, topped by encoder, that slides within a bushing which rotates within bearings. The bushing is capped with a urethane friction ring which works to prevent the piston from sliding as body pivots about either grip.

is presented. The function and design of ROCR's magnetic gripping mechanisms is outlined. Two, simple, climbing gaits are explained and discussed. These climbing gaits are then compared in simulation and the relative advantages of each gait are determined in terms of energy efficiency and control strategy. Optimal gaits are currently being implemented in the prototype.

II. Physical Layout, Design and Sensors

ROCR is a T-shaped, pendular two-link, serial chain robot with a pivoting tail attached to the bottom of the T (as shown in Fig. 1) and two gripping mechanisms, one at each end of the T's crossbar. The top of the T is 30.5 cm across, the swinging portion of the tail is 45.7 cm long and the joint location of the tail is adjustable such that it can be moved from 5-20 cm below the centerline between the robot's gripping mechanisms. ROCR's bio-inspired oscillating climbing strategy is the key to its efficient climbing gaits. ROCR alternately grips the wall with one hand at a time and swings its tail, causing a center of gravity shift that raises its free hand, which then grips the climbing surface as portrayed in Fig. 3. The hands swap gripping duties and ROCR swings its tail in the opposite direction. As ROCR's tail oscillates from side to side, the resultant center of gravity changes, which, coordinated with gripping activity, will drive the robot up a vertical surface.

A first generation ROCR prototype is shown in Fig. 2. This prototype incorporates encoders to measure body angle about the gripping hand as well as tail angle relative to ROCR's body. This encoder data is used to implement control strategies. ROCR is equipped with an IR rangefinder to help prevent collisions during climbing. Accelerometers attached to ROCR help compensate for sliding at the wall grips and sensor drift, and provide secondary position sensing for self calibration or swing recovery. Motion control and sensor analysis is performed in the onboard microcontroller and the tail motor is driven via the onboard h-bridge amplifier. To facilitate testing and demonstration, multiple climbing gaits and control strategies may be loaded into ROCR at the same time and switched between without reprogramming. ROCR's batteries are carried at the end of its tail since dead weight would otherwise be required at this location in order to produce the advantageous body torques, as the tail is swung, that are necessary to climb.

III. Magnetic Gripping Mechanisms

For the purposes of gait development and motion refinement, ROCR is fitted with magnetic gripping mechanisms. These magnetic grippers will yield more expedient experimental results than the other grippers being developed for ROCR and provide a proof of concept while investigating energy efficiency. Furthermore, there are many ferrous based surfaces worth climbing: radio towers, skyscrapers, oil rigs, etc. ROCR's modular design allows the substitution of a variety of gripping mechanisms, designed to climb non-ferrous surfaces, while still retaining the core functionality of ROCR's oscillating climbing strategy. Several microspine based designs, intended for use on walls with moderate surface roughness, have been investigated (e.g., [18]).

The gripping mechanism shown in Fig. 1 must be able to predictably and quickly engage and disengage the climbing surface. The body of ROCR must be able to pivot about an engaged gripping mechanism in order to reach upward with its disengaged mechanism. Sensor data must be readily available on the position of ROCR's body about its engaged gripping mechanism.

To accomplish these goals, a magnet-tipped piston, sliding inside a bushing, is located by bearings within a radially symmetric column. An optical encoder affixed to the piston provides rotational position data of the body of ROCR relative to the engaged gripping mechanism. A spring drives the piston into the engaged position, while remote control (RC) servos mounted to the body of ROCR (see Fig. 2) pull the magnet-tipped pistons into the disengaged position via cables. A urethane friction ring, located peripherally to the magnet, helps prevent the magnetic piston from sliding as ROCR pivots about the attached gripping mechanism.

IV. Initial Climbing Gaits

The pendular two-link design of ROCR dictates the method by which the robot will climb; however, many climbing gaits are possible. Different gaits engage and disengage the wall with their gripping mechanisms (or hands) at different times during the oscillatory swinging of the tail. Two preliminary climbing gaits were identified for ROCR prior to simulation and modeling and were selected for evaluation due to the ease of their practical implementation

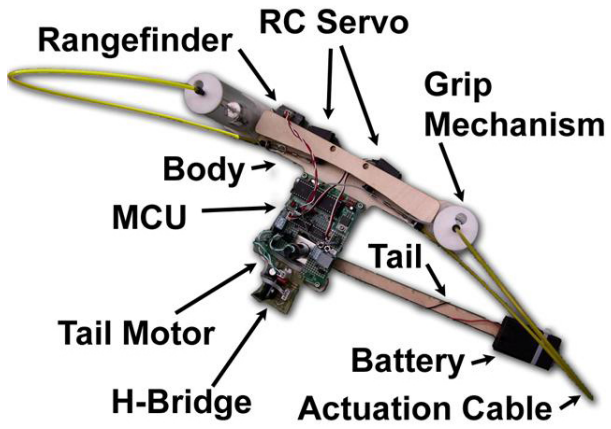

Fig. 2. Second generation prototype of ROCR, with RC servos, geared DC motor, grip mechanisms incorporating optical encoders for body angle measurement, onboard MCU and H-Bridge, and tail mounted battery.

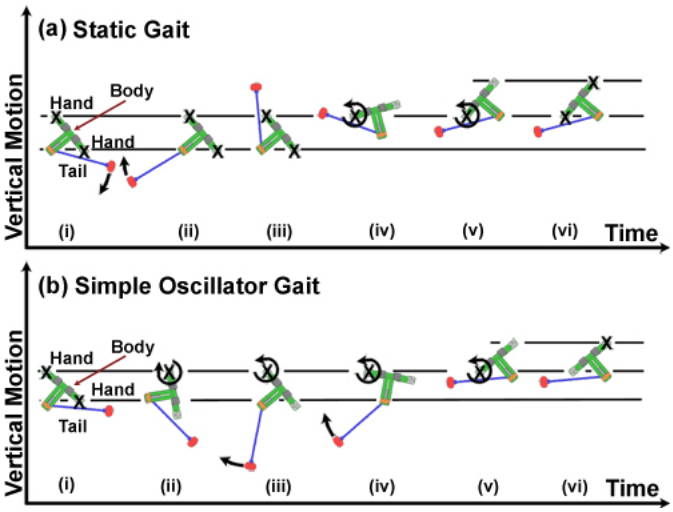

Fig. 3. Filmstrip style cartoons of climbing gaits for ROCR are shown above. Subsequent, numbered frames from left to right represent ROCR's body position shifts and resultant vertical progress (progress can be noted relative to horizontal lines). From top to bottom, gaits shown are Static (a) and Simple Oscillator (b). Engaged gripping mechanisms are shown as Xs, arrows indicate tail motion relative to robot body and body rotation about an engaged gripping mechanism.

on a microcontroller. They are named the Static gait and the Simple Oscillator gait (shown in Fig. 3). The Simple Oscillator gait can be controlled in several ways. Whereas in the static gait, control is based on the target position of the tail itself the Simple Oscillator control can be based on either the tail position or the frequency of the tail movements. The goal of the Simple Oscillator gait is to achieve a tuned resonant response for maximum efficiency as has been observed in other mechanical systems [28]. This work will use a tail oscillation frequency-based controller.

A. Static Gait

The Static gait, shown at the top of Fig. 3(a), is the simplest of the gait strategies. In this case, both hands grip the wall while the tail swings all the way to one side relative to the body, either completely to the left or to the right as indicated in Fig. 3)(a)(i-iii). This mass shifting provides the maximum offset of ROCR's center of gravity for maximum stored potential energy. Then, the hand that is furthest from the tail lets go (just after Fig. 3)(a)(iii)), providing a stepwise release of the stored potential energy and corresponding angular step response as indicated in Fig. 3(a)(iv). Ideally, the response of the robot is underdamped, providing ROCR the maximum body swing per stored energy potential. During the swing phase, the tail position relative to the body link is held constant. Upon attaining maximum vertical height of the free hand (Fig. 3(a)(v)), the free hand grips the wall (Fig. 3(a)(vi)), thus completing a single stride or half cycle. Next, the tail is driven to its opposite extreme position while both hands grip the wall and the sequence is repeated to complete a full cycle. This gait strategy requires the least time hanging onto the wall by only one hand. However, since the robot must lift its tail until it is at least orthogonal to the gravity vector (as is most obvious in Fig. 3)(a)(iii)), this gait requires a large amount of energy input to the tail motor. The static gait's simplicity makes it easily simulated as well as a natural starting point for the experimental evaluation of ROCR's climbing ability.

The logic implemented in simulating the static gait is very simple: the tail is moved until a desired tail angular position is achieved, then a grip is released and remains released until a maximum body angular position is achieved without flipping completely over at which point the free grip is engaged and the tail begins swinging in the opposite direction (see Fig. 4(a)). This logic accurately reproduces the static gait yet has one added feature that ensures optimal climbing rate. The simulation logic limits the body swing up response to a maximum limit of θ_{max} which corresponds to the angle of maximum reach of the body per body swing.

B. Simple Oscillator Gait

The Simple Oscillator gait, shown in Fig. 3(b), uses a more continuous motion than the Static gait, inputting energy (via tail swinging) as the body swings about a single hand. This dynamic gait makes more efficient use of input energy by allowing the motor to operate over a less energy intensive range of angles with respect to gravity than the static gait (i.e., the motor never has to lift the tail completely perpendicular to the ground). At the heart of this strategy is a sinusoidal forcing function that drives the tail motion with a prescribed amplitude and frequency in the spirit of previous climbing robot work [30], [19]. The robot exchanges hand holds as the prescribed tail motion reaches θ_{targ}, its right- and left-most maximum amplitude. This behavior is generally portrayed in Fig. 3(b). For practical purposes a torque saturation limit, τ_{max}, has also been instituted to reflect motor torque limits.

This gait is expected to impart lower lateral and twisting loads to the magnets in ROCR's hands and may permit lighter weight gripping mechanisms to be used. This gait also has the advantage that the tail never has to be lifted as high (orthogonal to gravity) relative to the Static gait. The Simple Oscillator will be more energy efficient than the

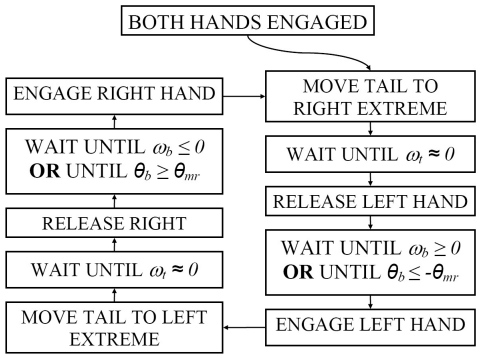

(a) Static

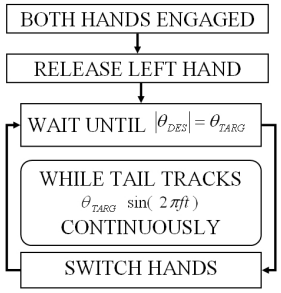

(b) Simple Oscillator

Fig. 4. Simulation logic used to produce ROCR's climbing gait strategies. θ_b is the angular position of the body, ω_b is the angular velocity of the body, θ_t is the relative angular position of the tail with respect the body, ω_t is the angular velocity of the tail, θ_{targ} is the amplitude of the input tail signal, f is the driving frequency of the tail input signal in Hz, "t" is the time in seconds, and θ_{mr} is the angle of maximum reach.

Static gait because of this. However, the frequency of the Simple Oscillator needs to be tuned in order to maximize its climbing ability as some tail input frequencies will result in less desirable climbing rates and energy efficiencies than others as shown in Table I.

The logic for the Frequency style of Simple Oscillator can be seen in Fig. 4(b). The desired tail reference signal can be tuned in terms of frequency and amplitude for the determination of optimal climbing parameters.

V. Simulation and Interpretation of Results

In order to evaluate the climbing strategies of ROCR and to fine tune the physical paremeters of the robot, a simulation model was produced based on the first ROCR prototype outlined in section II. The actual prototype dimensions were reproduced with six idealized lumped mass distributions of the major components (i.e., tail end mass, tail motor mass, hand servo motors, etc.) as shown in Fig. 5. The total body mass is 800 g with the tail mass, m_{tail}, representing 300 g of this. The simulation was developed in Working Model 2D with ROCR's actual parameters.

The efficiency of each of the climbing gaits was evaluated by computing the amount of input energy needed to achieve vertical climbing. This energy was calculated by numerically integrating the required tail power over time ($P = \tau \cdot \omega$). The effectiveness of each of the climbing strategies was

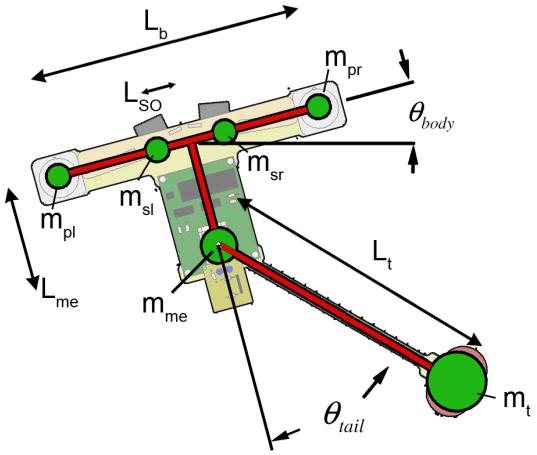

Fig. 5. Front view of ROCR overlayed with model mass distribution and showing model dimensions. Masses shown: m_t = 300 g is tail mass, m_{sl} = 22 g and m_{sr} = 22 g are left and right servo masses, m_{gl} = 58 g and m_{gr} = 58 g are left and right grip mechanism masses, m_{me} = 175 g is combined motor and electronics mass.

Gait Strategy	Θ_{Tar} (deg)	τ_{max} (Nm)	f $_{tail}$ (Hz)	Energy (J/m)	Energy Ratio	Rate (BL/s)
$\delta PE*$	N/A	N/A	N/A	7.8*	1.00	N/A
Static**	90	2.5	0.04	53.0	6.76	0.019
Static**	90	7.5	0.04	56.7	7.23	0.019
Simple Osc.	30	0.8	0.70	25.6	3.27	0.154
Simple Osc.	45	0.9	0.70	26.1	3.33	0.260
Simple Osc.	60	0.7	0.55	28.5	3.64	0.263
Simple Osc.	60	0.8	0.60	26.0	3.31	0.305
Simple Osc.	60	0.9	0.65	25.4	3.24	0.335
Simple Osc.	60	1.0	0.70	27.4	3.49	0.382
Simple Osc.	60	1.1	0.75	29.0	3.70	0.418
Simple Osc.	75	1.1	0.65	29.1	3.71	0.189
Simple Osc.	90	0.9	0.60	28.2	3.61	0.260

TABLE I

Climbing gait comparison in terms of tail frequency, maximum torque input and energy used. Lowest energy tail frequency is shown for each of a range of target tail angles. A range of motor torques and tail frequencies are shown for the most promising target tail angle of 60°. Freq. SO is frequency driven simple oscillator. BL=59.1 cm. Energy ratio is the ratio of the required energy for a specific gate divided by the increase in potential energy. *Potential energy is δPE = M*G*δh.

determined by comparing the amount of energy input into the system to the amount of potential energy gained (per meter). All simulations incorporated wall damping forces (0.0005 Nms/Rad) at the current hand pivot, assumed ideal tail motor efficiency, gearing efficiency, and wall adhesion in the energy calculations. For a valid comparison, these calculations are compared to the idealized potential energy gained while climbing (7.84 J/m), which was calculated using $\Delta PE = m_{robot} * g * \Delta h$. In order to more accurately compare the gaits to one another, simulations were run until steady-state climbing was achieved and then data was

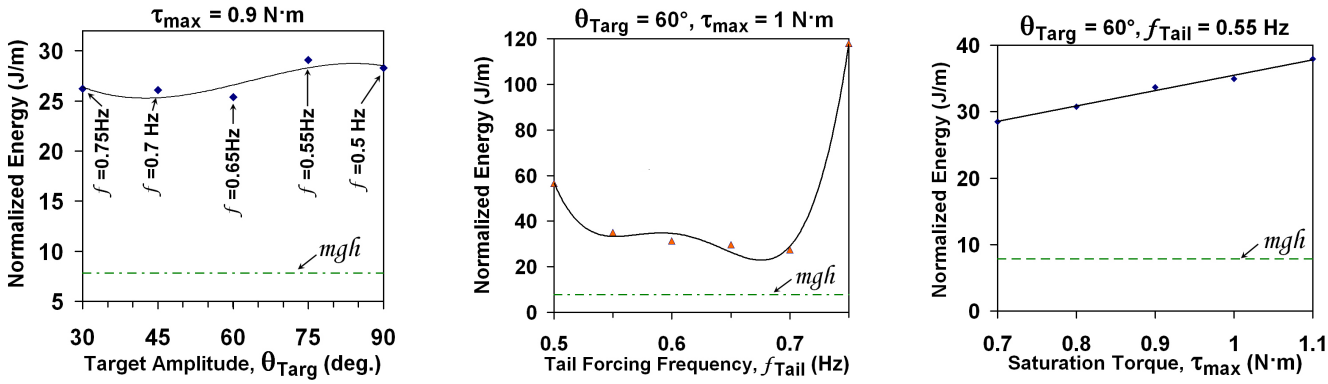

(a) Target Amplitude (b) Tail Forcing Frequency (c) Saturation Torque

Fig. 6. Minimum energy cases are presented for (a) Tail torque limited to τ_{max} = 0.9 Nm, (b) Tail amplitude of θ_{targ} = 60° and τ_{max} = 1 Nm and (c) θ_{targ} = 60° and tail forcing frequency of f_{tail} = 0.55 Hz

collected for a specific number of gait cycles.

Both climbing gaits were simulated and were subject to prescribed tail amplitudes, θ_{targ}, and torque saturation limits, τ_{max}. A torque limit was implemented to reflect the operating limitations of the prototype's RE16 motor. In the simulations, the forcing frequency of the tail, f_{tail} was varied over a small range above and below the expected resonance frequency, while also investigating the effect of tail amplitude, θ_{targ}, over a range of $\pm 30°$ to $\pm 90°$ and the effect of motor torque saturation, τ_{max}. The results of the simulations are shown in Table I. This table shows two different simulation scenarios. Typical simulation results for the Static gait can be seen in the second and third lines of the table. As expected, the Static gait is relatively inefficient costing approximately 7 times as much energy as the potential energy gained ($= m * g * \delta h$ as shown in the first row of Table I). This is because the tail must be lifted perpindicular to gravity. The energy efficiency of static gait is not very sensitive to variations in the maximum allowable tail torque. Note that during the swinging phase of the static gait, no energy is input to the system as the tail remains stationary relative to the body.

The Simple Oscillator gait results are located in the next nine lines of the table and show a minimum climbing energy cost of about 25.4 J/m occurring around tail amplitude $\theta_{targ} = 60°$, maximum tail torque 0.9 Nm and a tail frequency of 0.65 Hz. This represents a 52% reduction from the Static gait. One can also observe similar efficiences for tail amplitudes, $\theta_{targ} = 30°$ and 45° but a slightly higher forcing frequency, f_{tail} (see table I). This is fortuitous and suggests that careful tuning will not be neccessary to run ROCR effectively. Figures 6(b) and 6(c) provide further information for the 60° tail amplitude cases. Figure 6(c) shows an increasing trend in energy consumption with increasing saturation torque, τ_{max}, whereas Fig. 6(b) shows a local energy minimum at f_{tail} = 0.7 Hz when τ_{max} is held constant at 1 Nm. It is also informative to examine the data for θ_{targ} = 60° in Table I which shows the minimum energy case under torque saturation limits, τ_{max}, over the range 0.7-1.1 Nm. Note that the optimum forcing frequency is inversely proportional to these torque limits. This is intuitive since as we start to limit the torque, the tail and hence also the body, accelerates more slowly, so that staying at a high forcing frequency will not allow the robot to fully rotate to achieve maximum "reach". This behavior is also exhibited with increasing tail angle, θ_{targ}, and can be observed in Fig. 6(a).

As expected from our previous intuition, the results of the frequency driven simulations confirm that by driving ROCR near its natural frequency that a minimal amount of energy is required for efficient climbing. Also, by operating in this range of torques and frequencies, ROCR's current motor (a geared Maxon RE16 motor used to propel ROCRs tail) will be very suitable for further testing, staying below 10% of ROCRs tail motor stall torque to operate near maximum motor efficiency for the Simple Oscillator gait. This motor will also have the additional torque available that is necessary to investigate the Static gait.

VI. Conclusions and Future Work

We have presented the novel climbing robot ROCR. ROCR combines mass shifting observed in human climbers with a reoriented brachiative motion observed in swinging gibbons. ROCR's design and bio-inspired climbing strategy have been explained. This strategy requires just enough input energy to shift ROCR's center of mass in order to make vertical climbing progress. Initial climbing gaits have been outlined and simulation results validating these initial gaits have been shown. Simulation results confirm that by using a control strategy which drives ROCR's tail near its resonant frequency, even with low torques, efficient vertical climbing is achieved, requiring about half the energy of the Static gait. These results have guided the construction of a prototype capable of efficient climbing, using a simple mechanical design.

A prototype of ROCR has been built in order to test climbing gaits, including those already explored in simulation. This prototype was built with an emphasis on mechanical simplicity, energy efficiency, modularity, the ability to switch

between multiple gait strategies, and low autonomous weight. Magnetic tipped gripping mechanisms were constructed in order to streamline the initial proof of concept. These grippers are modular in design and the magnetic tips may be exchanged for other designs. A variety of non-magnetic bio-inspired gripping mechanisms are being developed which should enable ROCR to climb vertical walls with a range of surface roughness from sandstone to brick. Some of the promising microspine designs are passive, but force sensing material may permit an active microspine design. The development of suitable force sensing materials would enable such a design to be implemented using Shape Deposition Manufacturing (a rapid prototyping process involving a series of machining and deposition steps [29]).

Going forward, physical parameters of the current prototype, such as wall damping, will be incorporated into the model. The updated model will be validated experimentally through testing with the prototype to provide a more realistic simulation. Ultimately, ROCR provides an efficient and mechanically simple wall climbing platform for studying climbing motion inspired by a combination of human climber mass shifting and gibbon brachiation.

VII. ACKNOWLEDGMENTS

The authors wish to acknowledge Tom Slowik, Mike Knutson, and Keith Findling for help in fabricating.

REFERENCES

[1] C. von Alt, et al., "Hunting for mines with REMUS: a high performance, affordable, free swimming underwater robot," in OCEANS, 2001. MTS/IEEE Conference and Exhibition, 2001, pp. 117-122 vol.1.

[2] L. Briones, P. Bustamante and M. A. Serna, "Wall-climbing robot for inspection in nuclear power plants," Proceedings of IEEE ICRA 1994, pp. 1409-1414 vol.2.

[3] F. W. Bach, H. Haferkamp, J. Lindemaier and M. Rachkov, "Underwater climbing robot for contact arc metal drilling and cutting," in Industrial Electronics, Control, and Instrumentation, 1996., Proceedings of the 1996 IEEE IECON 22nd International Conference on, 1996, pp. 1560-1565 vol.3.

[4] C. Balaguer, et al.,"A climbing autonomous robot for inspection applications in 3d complex environments."' Robotica, 18:287-297, 2000.

[5] R. T. Pack, J. L. Christopher, Jr. and K. Kawamura, "A Rubbertuator-based structure-climbing inspection robot," Proceedings of IEEE ICRA 1997, pp. 1869-1874 vol.3.

[6] L. P. Kalra, S. Weimin and J. Gu, "A Wall Climbing Robotic System for Non Destructive Inspection of Above Ground Tanks," in Electrical and Computer Engineering, Canadian Conference on, 2006, pp. 402-405.

[7] S. Weihua, S. Yantao and X. Ning, "Mobile Sensor Navigation with Miniature Active Camera for Structure Inspection," in Intelligent Robots and Systems, 2006 IEEE/RSJ International Conference on, 2006, pp. 1177-1182.

[8] S. Liu, Y. Zhao, X. Gao, D. Xu and Y. Wang, "Wall climbing robot with magnetic crawlers for sand-blasting, spray-painting and measurement," Gaojishu Tongxin/High Technology Letters, vol. 10, pp. 86-88, 2000.

[9] C. Menon and M. Sitti, "Biologically Inspired Adhesion based Surface Climbing Robots," in IEEE ICRA, 2005, pp. 2715-2720.

[10] M. P. Murphy, W. Tso, M. Tanzini and M. Sitti, "Waalbot: An Agile Small-Scale Wall Climbing Robot Utilizing Pressure Sensitive Adhesives," Proceedings of IEEE/RSJ IROS 2006, pp. 3411-3416.

[11] R. Lal Tummala, et al., "Climbing the walls [robots]," Robotics and Automation Magazine, IEEE, vol. 9, pp. 10-19, 2002.

[12] Y. Zhao, Z. Fu, Q. Cao and Y. Wang, "Development and applications of wall-climbing robots with a single suction cup," Robotica, vol. 22, pp. 643-648, 2004.

[13] M. Sitti and R. S. Fearing, "Synthetic gecko foot-hair micro/nano-structures for future wall-climbing robots," Proceedings of IEEE ICRA 2003, pp. 1164-1170 vol.1.

[14] O. Unver, A. Uneri, A. Aydemir and M. Sitti, "Geckobot: a gecko inspired climbing robot using elastomer adhesives," Proceedings of IEEE ICRA 2006, pp. 2329-2335.

[15] B. E. Shores and M. A. Minor, "Design, Kinematic Analysis, and Quasi-Steady Control of a Morphic Rolling Disk Biped Climbing Robot," Proceedings of IEEE ICRA 2005, pp. 2721-2726.

[16] Q. Liu, "Magnetic adsorption type of wall-climbing robot was developed at Harbin Institute of Technology," Gaojishu Tongxin/High Technology Letters, vol. 6, p. 46, 1996.

[17] T. Sato, R. Fukui, H. Morishita and T. Mori, "Construction of ceiling adsorbed mobile robots platform utilizing permanent magnet inductive traction method," Proceedings of IEEE/RSJ IROS 2004, pp. 552-558 vol.1.

[18] S.Kim, A. T. Asbeck, M. R. Cutkosky and W. R. Provancher, "SpinybotII: climbing hard walls with compliant microspines," in Advanced Robotics, 2005. ICAR '05. Proceedings., 12th International Conference on, 2005, pp. 601-606.

[19] J. Clark, et al., "Design of a Bio-inspired Dynamical Vertical Climbing Robot," in Robotics: Science and Systems III Atlanta, Georgia, 2007.

[20] T. Bretl, S. Rock, and J.C. Latombe "Motion planning for a three-limbed climbing robot in vertical natural terrain." Proceedings of IEEE ICRA 2003.

[21] http://www.vortexhc.com/vmrp.html

[22] W. Shanqiang, L. Mantian, X. Shu and L. Yang, "A Wireless Distributed Wall Climbing Robotic System for Reconnaissance Purpose," in Mechatronics and Automation, Proceedings of the 2006 IEEE International Conference on, 2006, pp. 1308-1312.

[23] S. Kitai, K. Tsuru and S. Hirose, "The proposal of swarm type wall climbing robot system 'Anchor Climber'" Proceedings of IEEE IROS 2005, pp. 475-480.

[24] J. R. Usherwood and J. E. A. Bertram, "Understanding brachiation: insight from a collisional perspective." vol. 206, 2003, pp. 1631-1642.

[25] J. Nakanishi, T. Fukuda and D. E. Koditschek, "Preliminary studies of a second generation brachiation robot controller," Proceedings of IEEE ICRA 1997, pp. 2050-2056 vol.3.

[26] F. Saito, T. Fukuda and F. Arai, "Swing and locomotion control for two-link brachiation robot," Proceedings of IEEE ICRA 1993, pp. 719-724 vol.2.

[27] T. Henmi, D. Mingcong and A. Inoue, "Swing-up Control of the Acrobot Using a New Partial Linearization Controller Based on the Lyapunov Theorem," 2006, pp. 60-65.

[28] S. A. Bailey, J. G. Cham, M. R. Cutkosky and R. J. Full, "Comparing the Locomotion Dynamics of the Cockroach and a Shape Deposition Manufactured Biomimetic Hexapod," in Experimental Robotics VII, 2001, pp. 239-248.

[29] Weiss, L.E., et al., "Shape Deposition Manufacturing of Heterogenous Structures," Journal of Manufacturing Systems; 1997; v.16, no.4, p.239-248.

[30] D. I. Goldman, T. S. Chen, D. M. Dudek and R. J. Full, "Dynamics of rapid vertical climbing in cockroaches reveals a template," Journal of Experimental Biology, vol. 209, 2006.